

# Louvain-like Methods for Community Detection in Multiplex Networks

Sara Venturini\*, Andrea Cristofari†, Francesco Rinaldi‡, Francesco Tudisco§

**Abstract.** In this paper, we focus on the problem of community detection in multiplex networks, i.e., networks with multiple layers having same node sets and no intra-layer connections. In particular, we look for groups of nodes that can be recognized as communities consistently across the layers. To this end, we propose a new approach that generalizes the Louvain method by (a) simultaneously updating average and variance of the modularity scores across the layers, and (b) reformulating the greedy search procedure in terms of a filter-based multiobjective optimization scheme. Unlike many previous modularity maximization strategies, which rely on some form of aggregation of the various layers, our multiobjective approach aims at maximizing the individual modularities on each layer simultaneously. We report experiments on synthetic and real-world networks, showing the effectiveness and the robustness of the proposed strategies both in the informative case, where all layers show the same community structure, and in the noisy case, where some layers represent only noise.

**Key words.** community detection, multilayer networks, multiplex networks.

## 1 Introduction

Networks represented as graphs with nodes and edges have emerged as effective tools for modelling and analysing complex systems of interacting entities. In fact, graphs arise naturally in many disciplines, such as social networks [10], information networks [20], infrastructure networks [16], biological networks [8]. One of the most relevant issues in the analysis of graphs representing real systems is the identification of communities, i.e., groups of nodes that are densely connected to each other and loosely connected to the nodes in the other communities. While many community detection and clustering algorithms have been developed over the recent years, most of these are designed for standard single-layer graphs. On the other hand, having one single graph is often an oversimplifying assumption, which can lead to misleading models and results. Fortunato conducted a survey on this topic [15].

Advances in the study of networked systems have shown that the interconnected world is often composed of networks that are coupled to one another through different layers, where each layer represents one of many possible types of interactions. Multi-layer networks arise naturally in diverse applications such as transportation networks [17], financial-asset markets [1], temporal dynamics [44, 45], semantic world clustering [39], multivideo face analysis [6], mobile phone networks [19], social balance [7], citation analysis [43], and many others.

As for standard (single-layer) models, community detection is one key problem in the analysis of multi-layer networks and the presence of multiple layers poses several additional challenges. For instance, networks

---

\*Department of Mathematics “Tullio Levi-Civita”, University of Padova, 35121 Padova, Italy (sara.venturini@math.unipd.it)

†Department of Mathematics “Tullio Levi-Civita”, University of Padova, 35121 Padova, Italy (andrea.cristofari@unipd.it)

‡Department of Mathematics “Tullio Levi-Civita”, University of Padova, 35121 Padova, Italy (rinaldi@math.unipd.it)

§School of Mathematics, Gran Sasso Science Institute, Italy, (francesco.tudisco@gssi.it)

A. Cristofari, F. Rinaldi and F. Tudisco contributed equally to this work.

may have different types of multi-layer structures and communities may or may not be consistent across the layers.

Here, we focus on multiplex networks, modeled by a sequence of graphs (the layers) with a common set of nodes and no edges between nodes of different layers. We also assume that each layer is undirected and simple. Moreover, with the terminology introduced in [26], our aim is to find a set of communities that is *total* (i.e., every node belongs to at least one community), *node-disjoint* (i.e., no node belongs to more than one cluster on a single layer), and *pillar* (i.e., each node belongs to the same community across the layers). Several community detection algorithms for multiplex networks have been proposed in recent years. Among the successful approaches, we find methods that suitably reduce the multiplex to a single-layer graph, methods that are based on adaptations of single-layer consensus and spectral clustering, methods based on information-theoretic flow diffusion, and methods that infer communities by fitting suitable planted partition models. We attempt to summarize the related literature in §2 and refer to the survey [26] for further details.

In this paper, we propose a new strategy that directly approaches the multiobjective optimization problem of maximizing the modularity score of each individual layer. To this end, we adapt the popular Louvain heuristic method for single-layer networks [4], a locally greedy modularity-increasing sampling process over the set of node partitions. A natural extension of this method to the multiplex case, already studied in the literature, e.g. in [29, 1], is to locally maximize a weighted average  $M_Q$  of the modularity of the layers, instead of the modularity of a single layer. One of the advantages of using a linear combination of the layer modularities is that the increment of  $M_Q$  can be directly computed using the increment of the modularity of each layer, whose computation is efficiently handled by the original Louvain technique.

In a similar spirit, in §3 we consider a variant of the Louvain strategy which directly aims at maximizing the vector-valued function of the modularities of all the layers. To address the resulting multiobjective optimization problem, we propose a technique to memorize and dynamically update a list of several solutions, according to a suitably developed Pareto search. The size of the list as well as the final community assignment are controlled by means of a scalar cost function which takes into account for the variance of the layer modularities, on top of their average. The use of either a positive or a negative variance regularization term allows us to better control the amount of variability of the modularity scores across the layers and allows us to effectively handle both purely informative layers as well as the presence of noise. Moreover, while the resulting scalar cost function is a nonlinear combination of the layer modularities, we show that iteratively computing the modularity of each layer allows us to efficiently update their variance as well, resulting into an efficient variance-aware multiobjective Louvain-like scheme.

As such, an important feature of the proposed approach is that, unlike many methods presented in the literature, it does not need to preassign the number of classes at the beginning. This is particularly useful as we usually do not have information about the community structure of the multiplex and one must make some a-priori (possibly unjustified) assumption about the number of clusters otherwise.

To verify the performance and robustness of our technique, in our experimental set-up we study multiplex graphs in two settings: in the first one all layers are informative, i.e., all layers contain information about the community structure, whereas in the second setting at least one of the layers is a *noisy layer*, which accounts for corrupted measurements. In §4, we compare our method with nine baselines on synthetic multilayer networks generated via the Stochastic Block Model (SBM) [28] and the Lancichinetti-Fortunato-Radicchi (LFR) Benchmark [23], properly extended to the multiplex setting. Then, in §4.3, we compare the performance on several real-world multiplex graphs. Our results show that directly taking into account the variance across the layers may lead to much better performance, especially in the presence of noisy data. In particular, the proposed filter-based algorithm often leads to the best or second-best classification results, thus confirming the added value of the multiobjective approach.

## 2 Related work

In the following, we attempt to review and summarize some recent approaches to community detection for multi-layers. As in [26], we focus on algorithms explicitly designed to discover communities in multiplex networks.

Flattering methods reduce the multiplex network into a single-layer unweighted network and then apply a traditional community detection algorithm. The simplest algorithm of this type constructs a single-layer graph where two nodes are adjacent if they are neighbours in at least one layer [2]. An alternative is to create a weighted single-layer graph, where weights reflect some structural properties of the multiplex [2, 18].

Layer flattering coincides with summing the adjacency matrices of each layer into an aggregated adjacency matrix. More powerful community detection algorithms can be obtained, i.e., by merging modularity matrices or specific node embeddings. A study of these types of extensions is done in [41], with a novel method that integrates the layer-based node structural features.

Another popular approach is to perform aggregation at the cost function level, by extending single-layer community detection cost functions to the multilayer setting. The Generalized Louvain (GL) method proposed by Mucha et al. [29] is used to maximize a multilayer version of Newman’s modularity [30]. Bazzi et al. [1] propose a related approach with a Louvain-based modularity-maximization method for community detection in multilayer temporal networks. Both these approaches use a cross-layer modularity function that is essentially based on a weighted arithmetic mean of the modularities of the single layers. As we will discuss in the next section, our proposed approach defines a new variance-aware Louvain-like method, which leverage on this idea as starting point. A related approach is proposed by Pramanik et al. [37], where a weighted linear combination of the modularities of each layer is used to define a multilayer modularity index. Their approach focuses on the case of two-layer networks with both cross and within layer connections and aims at detecting cross-layer and within-layer communities simultaneously.

A variety of alternative strategies have been developed in relatively recent years. Pizzuti and Socievole [36] develop a genetic algorithm for community detection in multilayer networks that makes use of a multiobjective optimization formulation. In particular, the proposed algorithmic scheme exploits the concept of Pareto dominance when creating new populations at a given iteration, and returns a family of solutions that represent different trade-offs between the objectives at the end of the optimization process (the best solution is finally chosen using some tailored strategies).

De Domenico et al. [12] extend the famous information-theoretic approach of [38], by proposing a method that generalizes the so-called map equation for single graphs and identifies communities as group of nodes that capture flow dynamics within and across layers for a long time.

A method based on likelihood maximization is proposed by De Bacco et al. [11] for the setting of multilayer networks with possibly intra-layers couplings. They define a mixed-membership multilayer stochastic block model and propose a method that infers the communities by fitting this model to a given multilayer dataset via log-likelihood maximization.

Wilson et al. [46] propose a technique for multilayer data with intra-layer coupling that aims at identifying densely connected sets of vertex-layer pairs via a significance-based score that quantifies the connectivity of such sets as compared to a suitable fixed-degree random graph model.

Methods inspired by data clustering techniques are another popular line of work. Zeng et al. [49] proposed a pattern mining algorithm for finding closed quasi-cliques that appear on multiple layers with a frequency above a given threshold. A cross-graph quasi-clique is defined as a set of vertices belonging to a maximal quasi-clique that appears on all layers [34].

Tang et al. [43] and Dong et al. [14] proposed graph clustering algorithms for multilayer graphs based on matrix factorization. The key point is to extract common factors from multiple graphs to be used for various clustering methods. Tang et al. [43] factorize adjacency matrices while Dong et al. [14]

factorize graph Laplacian matrices. Liu et al. [25] proposed a nonnegative matrix factorization based multiview clustering algorithm, where the factors representing clustering structures from multiple views are regularized toward a common consensus.

Another popular line of research tries to extend spectral clustering to multilayer graphs. In general, these algorithms aim to define a graph operator that contains all the information of the multilayer graph such that the eigenvectors corresponding to the smallest eigenvalues are informative about the clustering structure. These methods usually rely on some sort of “mean operator”, e.g., the Laplacian of the average adjacency matrix or the average Laplacian matrix [33]. Further examples are the work of Zhou and Burges [53], which developed a multiview spectral clustering via generalizing the usual single view normalized cut to the multi-view case and tried to find a cut which is close to optimal on each layer, and the algorithm designed by Chen and Hero [9], which performs convex aggregation of layers based on signal-plus-noise models.

Alternative approaches are proposed for instance by Dong et al. [13], where spectral clustering is extended by merging the informative Laplacian eigenspaces of different layers via a subspace optimization analysis on Grassmann manifolds. Zhan et al. [50], [51], [52] developed several multiview graph learning approaches which merge multiple graphs into a unified graph with the desired number of connected components. Other multiview clustering approaches exploit the idea of maximizing clustering agreement. Zong et al. [54] introduced Weighted Multi-View Spectral Clustering, where the largest canonical angle is used to measure the difference between spectral clustering results of different views. Nie et al. [31] proposed a self-weighted scheme for fusing multiple graphs with the importance of each view considered, called Procrustes Analysis technique.

A common limitation of the proposed multiview clustering methods is that they do not consider to deal with possibly noisy or corrupted data, because they focus on the consistency of multiple layers and do not consider the inconsistency. To address this issue, Xia et al. [48] proposed Robust Multi-view Spectral Clustering, a Markov chain method that aims to learn an intrinsic transition matrix from multiple views by restricting the transition matrix to be low-rank. This aspect has also been considered by Mercado et al. [28], [27], where they propose a Laplacian operator obtained by merging the Laplacians from different layers via a one-parameter family of nonlinear matrix power means. Recently, Liang et al. [24] proposed a multiview graph learning framework, which simultaneously models multi-view consistency and multiview inconsistency in a unified objective function.

Another line of work adopts Bayesian inference [47], in which certain hypotheses about connections between nodes are made to find the best fit of a model to the graph through the optimization of a suitable likelihood [35].

Bickel and Scheffer [3] extended the semi-supervised co-training approach [5] to multi-view clustering. The basic idea of co-training is to iterate over all views and optimize the objective function in the next view using the result obtained from the latter one. A co-training approach is proposed by Kumar and Daumé [21], where the algorithm aims to find a consistent clustering that agrees across the views under the main assumption that all layers can be independently used for clustering. Under the same assumption, Kumar et al. [22] proposed Co-regularized Spectral Clustering, where they concentrated on this approach under the notion of co-regularization, maximizing the agreement between different views.

### 3 Multiobjective Louvain-like method for multiplex networks

In this section, we present our method for community detection in multiplex networks which, based on the popular Louvain heuristic method for single-layer networks [4], aims at maximizing the modularity of all layers simultaneously. Unlike many alternative strategies, where either the multiplex or the cost function are aggregated into a single-layer representative of the original multiple layers, our approach directly takes

into account the multiobjective nature of the problem under analysis, i.e., the existence of more than one objective to optimize. To this end, we maintain and update a list of suitable community assignments during the algorithm, each of them being preferable over the others with respect to a specific criterion. More formally, consider a multiplex with  $k$  layers  $G_1, \dots, G_k$ , where  $G_s = (V, E_s)$  is the graph forming the  $s$ -th layer. Thus, consider the vector of layer modularities  $Q = (Q_1, \dots, Q_k)$ , with the modularity score of the  $s$ -th layer defined as

$$Q_s = \frac{1}{2m_s} \sum_{ij} \left( A_{ij}^{(s)} - \frac{d_i^{(s)} d_j^{(s)}}{2m_s} \right) \delta(C_i, C_j) \quad (1)$$

where the sum runs over all pairs of vertices,  $A^{(s)}$  is the adjacency matrix of  $G_s$ ,  $m_s$  the total number of edges in  $E_s$  (or the sum of all their weights, in the case of weighted graphs),  $d_i^{(s)}$  is the degree (or weighted degree) of the node  $i$  in  $G_s$ ,  $C_i$  is the community node  $i$  belongs to, and the function  $\delta$  yields one if vertices  $i$  and  $j$  are in the same community (i.e.,  $C_i = C_j$ ) and zero otherwise.

We aim at maximizing all entries of  $Q$  simultaneously, i.e., we consider the following multiobjective optimization problem:

$$\max_{\{\text{partitions of } V\}} (Q_1, \dots, Q_k) \quad (2)$$

In multiobjective optimization, there is not a unique way to define optimality, since there is no a-priori total order for  $\mathbb{R}^k$  and each partial order leads to different strategies. Here, we consider the well-established definition of optimality according to Pareto [32]:

**Definition 3.1.** Given two vectors  $z^1, z^2 \in \mathbb{R}^k$ , we write  $z^1 \succeq_P z^2$  if  $z^1$  dominates  $z^2$  according to Pareto, that is:

$$\begin{aligned} z_i^1 &\geq z_i^2 && \text{for each index } i = 1, \dots, k \text{ and} \\ z_j^1 &> z_j^2 && \text{for at least one index } j = 1, \dots, k. \end{aligned}$$

A vector  $z^* \in \mathbb{R}^k$  is Pareto optimal if there is no other vector  $z \in \mathbb{R}^k$  such that  $z \succeq_P z^*$ . Moreover, the Pareto front is the set of all Pareto optimal points.

To address (2), we proceed by adapting the standard Louvain method with the aim of approaching a suitable candidate solution on the Pareto front of the modularity vector. To this end, we start with an initial partition where each node represents a community, to which corresponds the initial modularity vector  $Q$ . Then, we proceed with a two-phase scheme which generates a list  $L$  of community assignments and corresponding modularity vectors such that no one is Pareto-dominated by the others. The final approximate solution is then chosen in terms of a scalar function  $F$  used to assess the “quality” of a partition across the multiple layers. The choice of  $F$  is discussed in §3.1. To start with, the list  $L$  consists of the initial vector  $Q$ , the initial community partitioning and the corresponding value of  $F$ .

In the first phase, the algorithm picks one node at a time, following a given initial node ordering. For each node  $i$  and for every layer, we compute the modularity gain obtained by removing  $i$  from its community  $C_i$  and, for every neighbor  $j$  of node  $i$  (among the  $j$ s that have not been considered yet), we compute the modularity gain obtained by including  $i$  in the community  $C_j$ . For each such change of community assignment we evaluate the new modularity vector  $Q^{(i \rightarrow j)}$  by efficiently updating the previous modularity scores as in the original Louvain scheme. If  $Q^{(i \rightarrow j)}$  is not Pareto-dominated by any of the modularity vectors in  $L$ ,  $Q^{(i \rightarrow j)}$  is a good candidate to be added to  $L$ . However, as in the original Louvain method, we want to consider only new modularity vectors that yield a “strict improvement”. To this end, we use the modularity updates to efficiently evaluate the scalar function  $F$ . If additionally the new modularities  $Q^{(i \rightarrow j)}$  correspond to a positive increment of the quality function  $F$ , we add  $Q^{(i \rightarrow j)}$ , the new value of  $F$  and the corresponding partition to  $L$ . Thus, we remove from  $L$  all the partitions whose modularity vectors

are dominated by the newly inserted one. Moreover, in order to avoid the list computed this way to grow exponentially in size, we add a final control on the length of  $L$  by filtering out the elements of  $L$  that have small value of  $F$ , maintaining only the  $h$  partitions that achieve the largest value.

We proceed this way until the list stops changing and contains only vectors that do not dominate each other. At this point, the method selects from  $L$  the best partition with respect to  $F$  and uses this as new starting point. We then move to the second phase, which consists of an aggregation step where the communities in the selected partition are merged into single vertices, forming a smaller graph. The whole procedure is then repeated iteratively, until no further improvement in the Pareto sense is possible, in the same spirit of the original Louvain method for single-layer graphs. The overall scheme is summarized in Alg. 1.

Clearly, the choice of the function  $F$  may significantly affect the performance of the proposed strategy, both in terms of the final community assignment and in terms of computational time, as evaluating  $F$  may be an expensive operation. We argue below that a reasonable choice of  $F$  takes into account both average and variance of the layer modularities, and we show how these can be evaluated via an inexpensive iterative update.

### 3.1 Variance-aware cross-layer modularity function

One possibility to quantify the quality of a partition into communities for a multiplex is to measure the average of the corresponding modularity functions across all the layers. This corresponds to choosing  $F = M_Q$ , with

$$M_Q = \frac{1}{k} \sum_{s=1}^k Q_s. \quad (3)$$

The idea of considering a linear (possibly weighted) combination of the modularity functions of single layers is relatively natural and has been considered, for instance, in [1, 29, 37]. A key advantage of this choice is that the gain  $\Delta F_{i \rightarrow j}$ , measuring how the chosen function  $F$  changes when node  $i$  is moved from  $C_i$  to  $C_j$  during phase one of the algorithm, can be straightforwardly computed via linearity:

$$(\Delta M_Q)_{i \rightarrow j} = \frac{1}{k} \sum_{s=1}^k (\Delta Q_s)_{i \rightarrow j} \quad (4)$$

where  $(\Delta Q_s)_{i \rightarrow j}$  is the gain on modularity of layer  $s$  obtained when moving  $i$  from  $C_i$  to  $C_j$ . This observation is at the basis of the GL method, proposed in [29], see also [26, 1].

While the average yields a reasonable overview of the graph community structure across the layers, in many situations this may lead to an oversimplification [28, 27]. For instance, in the presence of noisy layers, linear averages over the multiple layers perform poorly [28]. To overcome this issue, we consider two functions that embed the sampled variance of the modularity of the layers:

$$F_- = (1 - \gamma)M_Q - \gamma V_Q, \quad (5)$$

$$F_+ = (1 - \gamma)M_Q + \gamma V_Q \quad (6)$$

where  $\gamma \in (0, 1)$  is a parameter and  $V_Q$  is the sampled variance of the modularity of the layers, which we compute as

$$V_Q = \frac{1}{k-1} \sum_{s=1}^k (Q_s - M_Q)^2. \quad (7)$$

It turns out that, as for the linear choice  $F = M_Q$ , the gain of both  $F_-$  and  $F_+$  can be computed in an efficient way during the algorithm via the updating formula

$$(\Delta F_{\pm})_{i \rightarrow j} = (1 - \gamma)(\Delta M_Q)_{i \rightarrow j} \pm \gamma R_Q,$$

where  $R_Q$  is defined as

$$R_Q = V_{\Delta Q} + \frac{2}{k-1}(Q - M_Q)^T(\Delta Q - \Delta M_Q),$$

$Q = (Q_1, \dots, Q_k)$  is the vector of layer modularities,  $\Delta Q$  is a vector whose  $s$ -th component is the gain  $(\Delta Q_s)_{i \rightarrow j}$ , and  $V_{\Delta Q}$  is the variance of  $\Delta Q$ , computed as follows:

$$V_{\Delta Q} = \frac{1}{k-1} \sum_{s=1}^k \{(\Delta Q_s)_{i \rightarrow j} - \Delta M_Q\}^2. \quad (8)$$

These formulas show that, as for  $M_Q$ , iteratively updating  $(\Delta Q_s)_{i \rightarrow j}$  allows us to iteratively update  $(\Delta F_{\pm})_{i \rightarrow j}$ . This allows us to evaluate the quality of the new community assignments and thus control the length of the list  $L$  by means of these variance-aware choices of the quality function  $F$  in a computationally efficient way.

### 3.2 Positive vs negative variance regularization

The quality functions  $F_+$  and  $F_-$  allow us to consider different types of variability of modularity across the layers. In particular, in the setting where all the layers have consistent community structure, we use  $F_-$ . The rationale behind this choice is that we want to obtain a trade-off between large modularity and sufficiently small variability in the layers (the larger  $\gamma$ , the smaller the variance in the final solution), which is what an ideal solution would look like if the community structure of all layers is in agreement. On the other hand, in the presence of some noisy layers, i.e., layers with no community structure,  $F_+$  is a better choice. In fact, in this case we want to favor solutions which have at the same time a good level of variability across the layers and a large enough modularity (the larger  $\gamma$ , the greater the level of allowed variability).

Overall, we study three variants of the proposed Louvain Multiobjective Method in Alg. 1, which correspond to the following three different choices of the function  $F$ : the modularity average  $M_Q$ , defined in (3), and the functions  $F_-$  and  $F_+$  defined in (5)–(6). We refer to the corresponding algorithms respectively as *Louvain Multiobjective Average (MA)*, *Louvain Multiobjective Variance Minus (MVM)* and *Louvain Multiobjective Variance Plus (MVP)*.

All these methods require to choose the length of the list  $L$ . The longer is such list, the better is the way we approach the Pareto front and explore the space related to the layer modularities. At the same time, this comes at a higher computational cost, which grows exponentially with  $h$ . Our experiments show that already  $h = 2, 3$  leads to remarkable performance, as compared to  $h = 1$ . We emphasize that, when we limit the length to  $h = 1$ , the method boils down to a form of aggregation strategy where the multiobjective approach is completely ignored and, instead, we aim at maximizing the chosen scalar function  $F$  by means of a Louvain-like greedy strategy. Thus, for example, MA with  $h = 1$  essentially corresponds to the GL method [29]. From this point of view, the methods MVP and MVM for  $h = 1$  are particularly interesting as they yield a variance-aware extension of the popular GL approach, whereas MA for  $h > 1$  provides a form of multiobjective GL. Moreover, when  $h = 1$ , the whole procedure of the method significantly simplifies. For these reasons, we use a separate notation for the case  $h = 1$ , referring to the method that uses the function  $F_-$  as *Louvain Expansion Variance Minus (EVM)* and to the method that uses the function  $F_+$  as *Louvain Expansion Variance Plus (EVP)*.

## 4 Experiments

We implemented the methods described in §3 using `Matlab`. Our codes are all available at the github page: <https://github.com/saraventurini/Louvain-like-Methods-for-Community-Detection-in-Multi-plex-Networks>.

---

**Algorithm 1** Louvain Multiobjective Method

---

**Input**  $G$  multiplex graph,  $F$  scalar quality function

**Output** final partition

$L$  initialized with node-based partition, the corresponding modularity vector  $Q$  and the value of  $F$

Set `terminate` = false

**repeat**

  Set `updateL` = true

**repeat**

**for all** node  $i$  of  $G$  **do**

**for all** partition  $C$  in list  $L$  **do**

        place  $i$  in every neighboring community which yields a positive increment of  $F$ . If the corresponding modularity vector  $Q$  is not Pareto-dominated by any of the modularity vectors in  $L$ , insert in  $L$  the vector  $Q$ , the corresponding partition and the  $F$  value. Delete from  $L$  all terms corresponding to modularity vectors that are dominated by  $Q$ .

**end for**

**end for**

    If  $L$  is longer than  $h$ , cut it to length  $h$  using  $F$

**if**  $L$  does not change **then**

`updateL` = false

**end if**

**until** (`updateL` == true)

  Consider the partition of the list  $L$  which maximizes the function  $F$  gain

**if**  $L$  has changed **then**

$G$  = reduced graph where each community of the selected partition is a node

**else**

    Set `terminate` = true

**end if**

**until** (`terminate` == true)

---

We considered both synthetic and real-world networks, performing extensive experiments to compare the proposed methods against nine multilayer community detection baselines (see §2 for details), namely:

- **GL**: Generalized Louvain [1, 29, 37];
- **CoReg**: Co-Regularized spectral clustering, with parameter  $\lambda = 0.01$  [22];
- **AWP**: Multi-view clustering via Adaptively Weighted Procrustes [31];
- **MCGC**: Multi-view Consensus Graph Clustering, with parameter  $\beta = 0.6$  [52];
- **PM**: Power mean Laplacian multilayer clustering, with parameter  $p = -10$  [28];
- **MT**: Multitensor expectation maximization [11];
- **SCML**: Subspace Analysis on Grassmann Manifolds, with parameter  $\alpha = 0.5$  [13];
- **PMM**: Principal Modularity Maximization, with parameters  $l = 10$  and  $\text{maxKmeans} = 5$  [42, 41];
- **IM**: Information-theoretic generalized map equation [12].



Notably, all these algorithms, except for GL and IM, require the user to specify the number of communities we look for a-priori. This is a potential drawback in practice, as we usually do not have information about the community structure of the graph and would have to make some (possibly unjustified) assumptions about the number of clusters.

Methods’ performance is evaluated using two metrics: the accuracy, measured as the percentage of nodes assigned to the correct community [52], and the Normalized Mutual Information (NMI) [40].

For all experiments, we considered two settings: the informative case, i.e., all the layers carry useful information about the underlying clusters, and the noisy case, where some of the layers are just randomly generated noise. As discussed in §3.1, a negative variance contribution as in  $F_-$  is suitable for the informative setting, while a positive variance term as in  $F_+$  may help in the presence of noisy layers. Thus, we test EVM and MVM for the informative case, while we use EVP and MVP in the noisy setting. Moreover, in order to confirm the advantages of the variance term in  $F_{\pm}$ , we further report the performance of MA, which only accounts for the sum of modularities across the layers (and thus provides a form of multiobjective version of GL). For the Louvain Multiobjective model, we consider the two list lengths  $h = 2, 3$  which we indicate by adding a number to the method’s acronym (e.g., MA2 stands for the Louvain Multiobjective Average method with list length  $h = 2$ ).

In order to evaluate the performance of the method as the variance regularizing parameter changes, we let  $\gamma \in \{0.1, 0.3, 0.5, 0.7, 0.9\}$  in the definition of  $F_-$  and  $F_+$ . In Figures 1-4 and Tables 1-3, we report the scores obtained with the parameter achieving the highest NMI on each dataset. However, a comparable performance is achieved for a large number of parameters, as shown in the Supplementary Material, where we report the performance of the methods as the parameter  $\gamma$  varies. In particular, this analysis provides an experimental guiding principle on the choice of  $\gamma$ , suggesting that a balanced contribution  $\gamma \approx 0.5$  is most appropriate in the informative setting, while a larger  $\gamma \approx 0.9$  seems to perform best in the presence of noise.

Being locally-greedy algorithms, the initial ordering of the nodes in phase one of all our methods may affect the final performance, just like the standard Louvain method. Based on our computational experience, it seems that choosing a specific ordering has a minor effect on the cost function itself, while it may have an impact on the computational time. Choosing the appropriate initial ordering is a nontrivial question and a well-known issue of this type of greedy strategies. In our experiments, we choose the initial ordering depending on the specific network setting we deal with. More specifically, we order the nodes according to the community size in the informative setting, while we list the nodes in random order in the noisy setting. This is mainly due to computational reasons: sorting the nodes according to the size of the corresponding community is indeed more expensive than assigning a random order. The sorting cost is reasonable in the experiments for the informative case, while it becomes prohibitive for the noisy case.

#### 4.1 Synthetic Networks via SBM

We consider here networks generated via the (multi-layer) Stochastic Block Model (SBM), a generative model for graphs with planted communities generated through the parameters  $p$  and  $q$ . These parameters represent the edge probabilities: given nodes  $i$  and  $j$ , the probability of observing an edge between them is  $p$  (resp.  $q$ ), if  $i$  and  $j$  belong to the same (resp. different) cluster.

We set  $p > q$  in order to generate synthetic informative layers, while we simply let  $p = q$  for the noisy ones. More precisely, we created networks with 4 communities of 125 nodes each and with  $k = 2, 3$  layers, by fixing  $p = 0.1$  and varying the ratio  $p/q$  in the generation of the informative layers. In the noisy layers, we fixed  $p = q = 0.1$ . For each value of the pair  $(p, q)$  we sample 10 random instances and we report average scores. Results are shown in Figures 1 and 2, where we consider the following four settings: 1(a) two informative layers; 1(b) three informative layers; 2(a) two informative layers and one noisy layer; 2(b) two informative layers and two noise ones. In general, our proposed approaches show good performance in

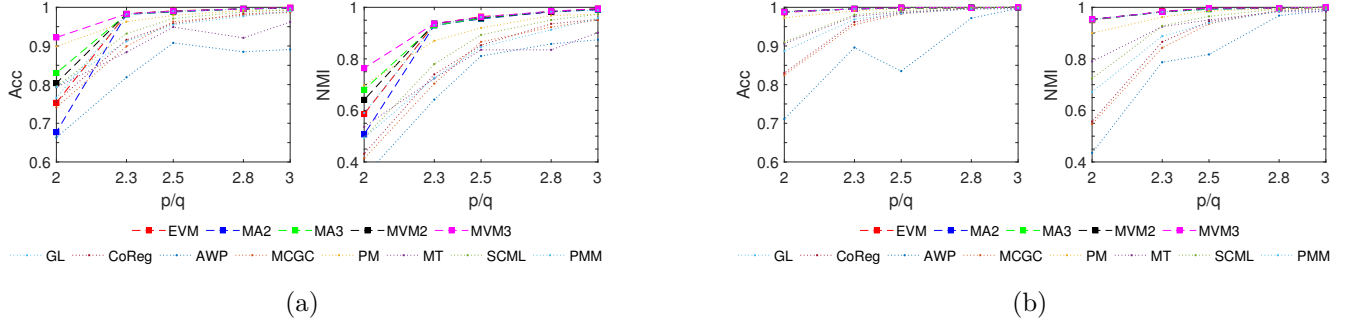


Figure 1: Average values of accuracy and NMI over 10 random networks sampled from SBM with equally distributed informative layers (2 layers (a) and 3 layers (b)) with four clusters of equal size, for  $p = 0.1$  and  $p/q \in \{2, 2.3, 2.5, 2.8, 3\}$ .

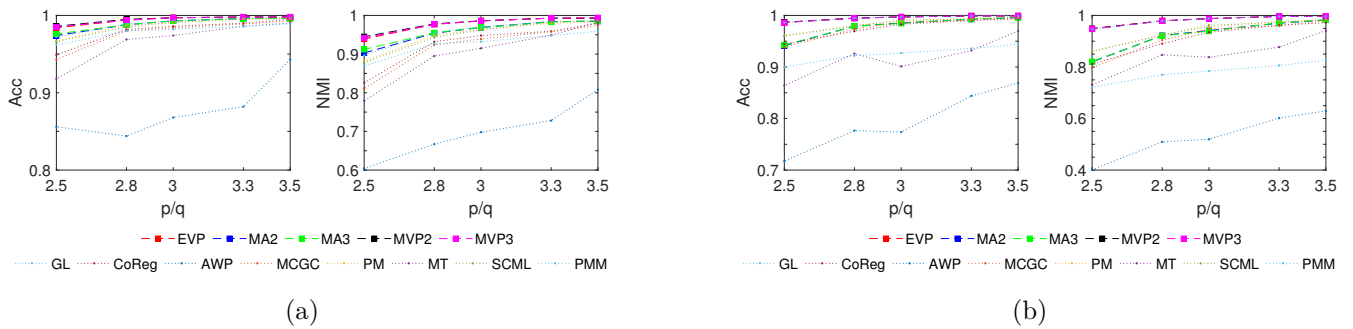


Figure 2: Average values of accuracy and NMI over 10 random networks sampled from SBM with both informative and noisy layers (two informative and one noisy in (a); two informative and two noisy in (b)). The informative layers are equally distributed SBM graphs with four clusters of equal size,  $p = 0.1$  and  $p/q \in \{2.5, 2.8, 3, 3.3, 3.5\}$ . The noisy layers are SBM graphs with  $p = q = 0.1$ .

almost all parameter settings, as compared to the baselines, and overall the variance-based multiobjective approaches (MVM and MVP) perform best, reaching very high accuracy and NMI even in the presence of two noisy layers (Fig. 2(b)). It is also interesting to notice that, while the community detection problem becomes easier when the ratio  $p/q$  grows, our proposed approaches still show performance advantages in that setting. In order to verify how the difference in the size of the communities can influence the performance, we tested the methods on networks with communities of different sizes. Similar results are observed in this setting, as reported in the Supplementary Material.

## 4.2 Synthetic Networks via LFR

Our second test setting is on synthetic networks generated via the Lancichinetti-Fortunato-Radicchi (LFR) benchmark [23], which allows us to model networks with more heterogeneous node degrees and community sizes than the SBM. We extended this benchmark to the multi-layer case, generating an independent network for each layer, using the same parameters. In particular, following [12], we considered graphs with 128 nodes and 4 communities, each with 32 nodes with average degree 16 and maximum degree 32. We let the fraction of inter-community links  $\mu$  vary. For the noisy layers, we forced the network to have just one community and we fixed  $\mu = 0$ , as suggested by the authors. As for the SBM, in our experiments we consider different combinations of informative and noisy layers. Results are shown in Figures 3 and 4, where the different pairs of panels correspond to accuracy and NMI for the settings: 3(a)

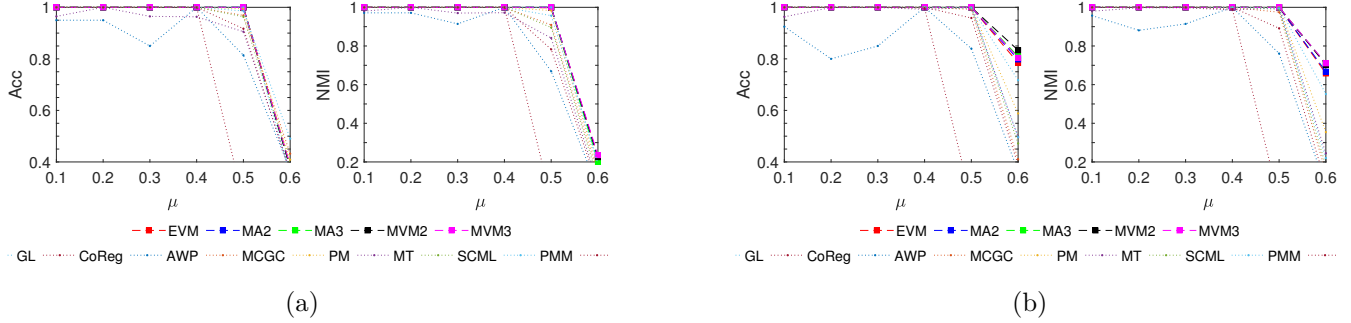


Figure 3: Average values of accuracy and NMI over 10 random networks sampled from LFR with equally distributed informative layers (2 layers (a) and 3 layers (b)), with four clusters and  $\mu \in \{0.1, 0.2, 0.3, 0.4, 0.5, 0.6\}$ .

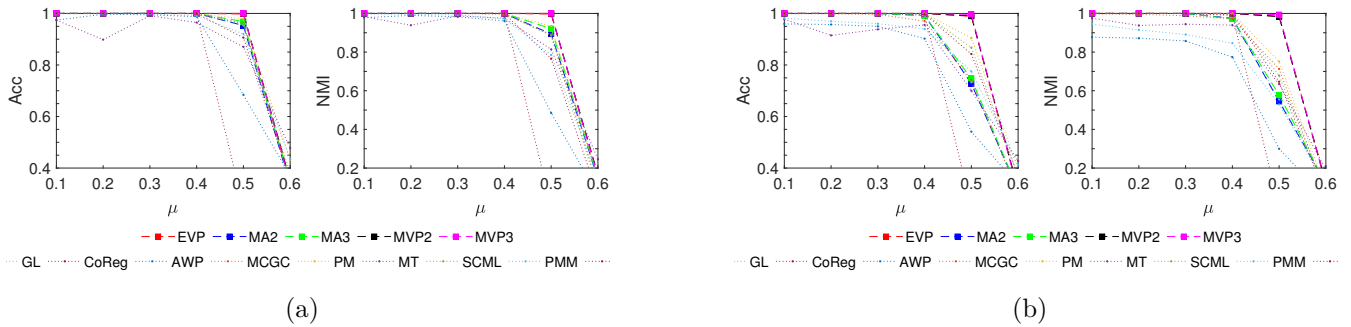


Figure 4: Average values of accuracy and NMI over 10 random networks sampled from LFR with both informative and noisy layers (two informative and one noisy in (a); two informative and two noisy in (b)). The informative layers are equally distributed LFR graphs with four clusters and  $\mu \in \{0.1, 0.2, 0.3, 0.4, 0.5, 0.6\}$ . The noisy layers are LFR graphs with one community and  $\mu = 0$ .

two informative layers; 3(b) three informative layers; 4(a) two informative layers and one noisy layer; 4(b) two informative layers and two noise ones. We can observe that the proposed methods give high values of both accuracy and NMI overall and are very competitive with respect to the baseline approaches. It is important to highlight that when  $\mu = 0.6$ , each node has more neighbors in other communities than in its own community, thus communities are no longer well-defined. This is the reason why all the methods struggle to find a good solution in that case.

### 4.3 Real World Networks

We consider five real-world datasets frequently used for evaluation in multilayer graph clustering, [28]: *3sources*, *BBCSport*, *Cora*, *UCI* and *Wikipedia*. A detailed description of these datasets is reported in the Supplementary Material.

Given the ground truth community structure of the graphs, we analysed both the informative and the noisy case. For the noisy case, we study two settings. In the first one, we added a noisy layer to the informative layers, whereas in the second setting we considered networks with 2 layers, where the first one is the graph obtained aggregating all the layers and the other one is just noise. The noisy layers are generated via uniform (Erdős–Rényi) random graphs with edge probability  $p \in \{0.01, 0.03, 0.05\}$ . For each value of  $p$ , and each dataset, we generated 10 random instances and for each instance we run our methods 10 times with different random initial community orderings.

Table 1: Real-world dataset setting one: no noisy layers. Average accuracy, NMI and performance ratio scores over 10 random initializations. All layers are informative. Best and second best values are highlighted with gray boxes.

	3sources		BBCSport		cora		UCI		Wikipedia		Perf. Ratios	
	Acc	NMI	Acc	NMI	Acc	NMI	Acc	NMI	Acc	NMI	$\rho_{Acc}$	$\rho_{NMI}$
EVM	0.876	0.789	0.833	0.798	<b>0.617</b>	<b>0.537</b>	0.882	0.921	0.548	0.520	0.951	<b>0.966</b>
MA2	0.858	0.749	0.899	0.825	0.407	0.434	0.753	0.862	0.525	0.521	0.863	0.912
MA3	0.876	0.789	0.596	0.731	0.425	0.428	0.876	0.910	0.558	0.546	0.838	0.920
MVM2	<b>0.888</b>	<b>0.812</b>	0.844	0.784	0.597	0.514	0.883	<b>0.925</b>	0.544	0.508	0.952	0.959
MVM3	<b>0.888</b>	<b>0.812</b>	0.915	<b>0.851</b>	0.603	0.502	0.883	<b>0.925</b>	0.530	0.504	<b>0.966</b>	0.965
GL	0.858	0.749	0.748	0.753	0.523	0.520	0.877	0.913	0.556	0.544	0.904	0.947
CoReg	0.651	0.658	0.858	0.617	0.530	0.380	<b>0.958</b>	0.911	0.522	0.445	0.905	0.840
AWP	0.686	0.662	0.616	0.722	0.534	0.293	0.869	0.891	0.462	0.332	0.843	0.758
MCGC	0.544	0.595	<b>0.919</b>	0.795	0.273	0.034	0.898	0.855	0.221	0.135	0.676	0.580
PM	0.734	0.707	0.778	0.690	0.551	0.456	0.876	0.879	<b>0.569</b>	<b>0.560</b>	0.896	0.892
MT	0.651	0.610	0.748	0.656	0.453	0.289	0.553	0.666	0.342	0.229	0.692	0.638
SCML	0.686	0.661	0.864	0.767	0.616	0.447	0.862	0.872	0.560	0.535	0.919	0.889
PMM	0.692	0.666	0.518	0.514	0.336	0.238	0.638	0.662	0.417	0.302	0.658	0.625
IM	0.539	0.624	0.531	0.401	0.431	0.477	0.721	0.761	0.123	0.11	0.570	0.630

Table 2: Real-world dataset setting two: informative layers plus one noisy layer. Average accuracy, NMI and performance ratio scores over 10 random initializations and 10 random edge probabilities  $p \in \{0.1, 0.3, 0.5\}$  for the noisy layer. Best and second best values are highlighted with gray boxes.

	3sources		BBCSport		cora		UCI		Wikipedia		Perf. Ratios	
	Acc	NMI	Acc	NMI	Acc	NMI	Acc	NMI	Acc	NMI	$\rho_{Acc}$	$\rho_{NMI}$
EVP	0.703	0.649	0.825	<b>0.797</b>	0.541	0.517	0.880	0.916	0.577	<b>0.556</b>	0.964	0.988
MA2	0.692	0.609	0.790	0.761	0.551	0.519	0.881	0.920	0.558	0.518	0.950	0.955
MA3	0.683	0.612	0.789	0.758	0.549	0.519	0.881	0.921	0.559	0.518	0.947	0.955
MVP2	0.717	0.668	0.828	<b>0.797</b>	0.543	0.518	0.881	0.920	0.578	0.555	0.970	0.994
MVP3	<b>0.730</b>	<b>0.677</b>	0.817	0.792	0.543	0.520	0.881	0.919	<b>0.579</b>	<b>0.556</b>	<b>0.971</b>	<b>0.996</b>
GL	0.678	0.607	0.777	0.754	<b>0.555</b>	<b>0.521</b>	0.881	0.920	0.561	0.520	0.945	0.953
CoReg	0.652	0.650	<b>0.849</b>	0.753	0.407	0.191	0.957	0.912	0.435	0.324	0.874	0.767
AWP	0.658	0.602	0.737	0.593	0.411	0.123	0.924	0.897	0.410	0.266	0.835	0.662
MCGC	0.546	0.585	0.812	0.694	0.303	0.005	0.804	0.816	0.201	0.107	0.686	0.563
PM	0.714	0.658	0.730	0.645	0.548	0.444	0.876	0.880	0.568	<b>0.556</b>	0.943	0.916
MT	0.624	0.627	0.519	0.355	0.187	0.011	0.660	0.723	0.170	0.051	0.556	0.453
SCML	0.639	0.593	0.772	0.604	0.222	0.028	<b>0.964</b>	<b>0.930</b>	0.185	0.057	0.701	0.558
PMM	0.538	0.508	0.387	0.167	0.255	0.060	0.667	0.677	0.172	0.047	0.528	0.377
IM	0.538	0.624	0.531	0.401	0.431	0.477	0.721	0.761	0.123	0.110	0.620	0.671

In Tables 1–3 we report the average accuracy and NMI scores over the samples and the random initializations. The best and second best values are highlighted with a gray box, with the best values having a bold font. We further consider the average performance ratio score values  $\rho_{Acc}$  and  $\rho_{NMI}$ , quantified as follows: for a given measure  $M_{a,d}$  (where  $M_{a,d}$  is either accuracy or NMI obtained by algorithm  $a$  over the dataset  $d$ ), the *performance ratio* is  $r_{a,d} = M_{a,d} / \max\{M_{a,d} \text{ over all } a\}$ . The average performance ratios of each algorithm  $\rho_{Acc}$  and  $\rho_{NMI}$  (for accuracy and NMI, respectively) are then obtained averaging  $r_{a,d}$  over all the datasets  $d$ . The closer is the average performance ratio of an algorithm to 1, the better will be the overall performance of that algorithm.

We can see that in many cases the proposed methods overcome the baselines. In particular, the methods that consider the variance in addition to the average of the modularity across the layers usually work better, with the multiobjective approaches MVM and MVP achieving the best results in almost all cases. This is in agreement with the more sophisticated Pareto-based strategy and is consistent with what observed in the experiments with synthetic data. Moreover, the last two tables highlight the robustness of the proposed methods with respect to noise. In fact, in the presence of noisy layers, the proposed methods — in particular the multiobjective ones — achieve very high performance ratios as well as overall high values of accuracy and NMI.

Table 3: Real-world dataset setting three: one aggregated informative layer plus one noisy layer. Average accuracy, NMI and performance ratio scores over 10 random initializations and 10 random edge probabilities  $p \in \{0.1, 0.3, 0.5\}$  for the noisy layer. Best and second best values are highlighted with gray boxes.

	3sources		BBCSport		cora		UCI		Wikipedia		Perf. Ratios	
	Acc	NMI	Acc	NMI	Acc	NMI	Acc	NMI	Acc	NMI	$\rho_{Acc}$	$\rho_{NMI}$
EVP	0.655	0.575	0.886	0.799	0.550	0.432	0.869	0.903	0.556	0.526	0.938	0.943
MA2	0.348	0.217	0.664	0.555	0.541	0.418	0.853	0.890	0.431	0.361	0.761	0.717
MA3	0.332	0.207	0.659	0.550	0.537	0.416	0.858	0.893	0.427	0.359	0.754	0.711
MVP2	0.744	0.675	0.914	0.826	0.546	0.430	0.872	0.905	0.564	0.538	0.969	0.980
MVP3	0.754	0.689	0.914	0.828	0.544	0.431	0.873	0.906	0.566	0.540	0.969	0.984
GL	0.327	0.203	0.664	0.549	0.537	0.418	0.866	0.898	0.427	0.360	0.756	0.713
CoReg	0.566	0.436	0.608	0.338	0.435	0.190	0.761	0.642	0.446	0.305	0.753	0.542
AWP	0.549	0.416	0.644	0.376	0.444	0.179	0.750	0.622	0.439	0.292	0.754	0.531
MCGC	0.512	0.479	0.682	0.480	0.276	0.020	0.702	0.691	0.347	0.291	0.654	0.514
PM	0.512	0.363	0.729	0.658	0.569	0.414	0.834	0.828	0.457	0.360	0.831	0.764
MT	0.693	0.614	0.729	0.614	0.272	0.113	0.634	0.699	0.406	0.306	0.714	0.534
SCML	0.514	0.410	0.797	0.661	0.600	0.416	0.846	0.835	0.479	0.365	0.867	0.783
PMM	0.440	0.304	0.424	0.206	0.311	0.108	0.641	0.535	0.386	0.249	0.591	0.392
IM	0.793	0.742	0.730	0.751	0.323	0.376	0.199	0.338	0.496	0.532	0.687	0.827

## 5 Conclusions

In this paper, we presented a new method for community detection in multiplex graphs that extend the Louvain heuristic method by introducing a variance-aware quality function and by performing a vector-valued modularity ascending scheme based on a tailored Pareto search.

We considered different versions of this method to better analyze two situations: the informative case, where each layer shows the same community structure, and the noisy case, where some layers present a community structure and all the others are just noise. We provided extensive experiments comparing with nine baselines borrowed from both the network science and the machine learning communities. We tested the performance of the proposed methods on synthetic networks, using the LFR and the stochastic block models, as well as five real-world multilayer datasets. In both cases, we studied informative and noisy settings. The experimental results demonstrate that the proposed method is competitive with the baselines. In particular, the multiobjective approach combined with the modularity variance shows the best performance in almost all cases.

## References

- [1] Marya Bazzi et al. “Community detection in temporal multilayer networks, with an application to correlation networks”. In: *Multiscale Modeling & Simulation* 14.1 (2016), pp. 1–41.
- [2] Michele Berlingerio, Michele Coscia, and Fosca Giannotti. “Finding and characterizing communities in multidimensional networks”. In: *2011 international conference on advances in social networks analysis and mining*. IEEE, 2011, pp. 490–494.
- [3] Steffen Bickel and Tobias Scheffer. “Multi-view clustering.” In: *ICDM*. Vol. 4. 2004. Citeseer, 2004, pp. 19–26.
- [4] Vincent D Blondel et al. “Fast unfolding of communities in large networks”. In: *Journal of statistical mechanics: theory and experiment* 2008.10 (2008), P10008.
- [5] Avrim Blum and Tom Mitchell. “Combining labeled and unlabeled data with co-training”. In: *Proceedings of the eleventh annual conference on Computational learning theory*. 1998, pp. 92–100.
- [6] Xiaochun Cao et al. “Constrained multi-view video face clustering”. In: *IEEE Transactions on Image Processing* 24.11 (2015), pp. 4381–4393.

- [7] Dorwin Cartwright and Frank Harary. “Structural balance: a generalization of Heider’s theory.” In: *Psychological review* 63.5 (1956), p. 277.
- [8] Jingchun Chen and Bo Yuan. “Detecting functional modules in the yeast protein–protein interaction network”. In: *Bioinformatics* 22.18 (2006), pp. 2283–2290.
- [9] Pin-Yu Chen and Alfred O Hero. “Multilayer spectral graph clustering via convex layer aggregation: Theory and algorithms”. In: *IEEE Transactions on Signal and Information Processing over Networks* 3.3 (2017), pp. 553–567.
- [10] James Samuel Coleman. *An Introduction to Mathematical Sociology*. Collier-Macmillan, London, UK, 1964.
- [11] Caterina De Bacco et al. “Community detection, link prediction, and layer interdependence in multilayer networks”. In: *Physical Review E* 95.4 (2017), p. 042317.
- [12] Manlio De Domenico et al. “Identifying modular flows on multilayer networks reveals highly overlapping organization in interconnected systems”. In: *Physical Review X* 5.1 (2015), p. 011027.
- [13] Xiaowen Dong et al. “Clustering on multi-layer graphs via subspace analysis on Grassmann manifolds”. In: *IEEE Transactions on signal processing* 62.4 (2013), pp. 905–918.
- [14] Xiaowen Dong et al. “Clustering with multi-layer graphs: A spectral perspective”. In: *IEEE Transactions on Signal Processing* 60.11 (2012), pp. 5820–5831.
- [15] Santo Fortunato. “Community detection in graphs”. In: *Physics reports* 486.3-5 (2010), pp. 75–174.
- [16] Riccardo Gallotti and Marc Barthelemy. “The multilayer temporal network of public transport in Great Britain”. In: *Scientific data* 2.1 (2015), pp. 1–8.
- [17] Riccardo Gallotti and Marc Barthelemy. “The multilayer temporal network of public transport in Great Britain”. In: *Scientific data* 2.1 (2015), pp. 1–8.
- [18] Jungeun Kim, Jae-Gil Lee, and Sungsu Lim. “Differential flattening: A novel framework for community detection in multi-layer graphs”. In: *ACM Transactions on Intelligent Systems and Technology (TIST)* 8.2 (2016), pp. 1–23.
- [19] Niko Kiukkonen et al. “Towards rich mobile phone datasets: Lausanne data collection campaign”. In: *Proc. ICPS, Berlin* 68 (2010).
- [20] Balachander Krishnamurthy and Jia Wang. “On network-aware clustering of web clients”. In: *Proceedings of the conference on Applications, Technologies, Architectures, and Protocols for Computer Communication*. 2000, pp. 97–110.
- [21] Abhishek Kumar and Hal Daumé. “A co-training approach for multi-view spectral clustering”. In: *Proceedings of the 28th international conference on machine learning (ICML-11)*. 2011, pp. 393–400.
- [22] Abhishek Kumar, Piyush Rai, and Hal Daume. “Co-regularized multi-view spectral clustering”. In: *Advances in neural information processing systems*. 2011, pp. 1413–1421.
- [23] Andrea Lancichinetti, Santo Fortunato, and Filippo Radicchi. “Benchmark graphs for testing community detection algorithms”. In: *Physical review E* 78.4 (2008), p. 046110.
- [24] Youwei Liang et al. “Multi-view Graph Learning by Joint Modeling of Consistency and Inconsistency”. In: *arXiv preprint arXiv:2008.10208* (2020).
- [25] Jialu Liu et al. “Multi-view clustering via joint nonnegative matrix factorization”. In: *Proceedings of the 2013 SIAM International Conference on Data Mining*. SIAM. 2013, pp. 252–260.
- [26] Matteo Magnani et al. “Community detection in multiplex networks”. In: *ACM Computing Surveys (CSUR)* 54.3 (2021), pp. 1–35.

- [27] Pedro Mercado, Francesco Tudisco, and Matthias Hein. “Generalized matrix means for semi-supervised learning with multilayer graphs”. In: *Advances in Neural Information Processing Systems*. 2019, pp. 14877–14886.
- [28] Pedro Mercado et al. “The power mean Laplacian for multilayer graph clustering”. In: *arXiv preprint arXiv:1803.00491* (2018).
- [29] Peter J Mucha et al. “Community structure in time-dependent, multiscale, and multiplex networks”. In: *science* 328.5980 (2010), pp. 876–878.
- [30] Mark EJ Newman. “Modularity and community structure in networks”. In: *Proceedings of the national academy of sciences* 103.23 (2006), pp. 8577–8582.
- [31] Feiping Nie, Lai Tian, and Xuelong Li. “Multiview clustering via adaptively weighted procrustes”. In: *Proceedings of the 24th ACM SIGKDD international conference on knowledge discovery & data mining*. 2018, pp. 2022–2030.
- [32] Vilfredo Pareto. “Cours d’économie politique, Rouge”. In: *Lausanne, Switzerland* (1896).
- [33] Subhadeep Paul and Yuguo Chen. “Spectral and matrix factorization methods for consistent community detection in multi-layer networks”. In: *The Annals of Statistics* 48.1 (2020), pp. 230–250.
- [34] Jian Pei, Daxin Jiang, and Aidong Zhang. “On mining cross-graph quasi-cliques”. In: *Proceedings of the eleventh ACM SIGKDD international conference on Knowledge discovery in data mining*. 2005, pp. 228–238.
- [35] Tiago P Peixoto. “Bayesian stochastic blockmodeling”. In: *Advances in network clustering and blockmodeling* (2019), pp. 289–332.
- [36] Clara Pizzuti and Annalisa Socievole. “Many-objective optimization for community detection in multi-layer networks”. In: *2017 IEEE Congress on Evolutionary Computation (CEC)*. IEEE. 2017, pp. 411–418.
- [37] Soumajit Pramanik et al. “Discovering community structure in multilayer networks”. In: *2017 IEEE International Conference on Data Science and Advanced Analytics (DSAA)*. IEEE. 2017, pp. 611–620.
- [38] Martin Rosvall and Carl T Bergstrom. “Maps of random walks on complex networks reveal community structure”. In: *Proceedings of the national academy of sciences* 105.4 (2008), pp. 1118–1123.
- [39] Joao Sedoc et al. “Semantic word clusters using signed spectral clustering”. In: *Proceedings of the 55th Annual Meeting of the Association for Computational Linguistics (Volume 1: Long Papers)*. 2017, pp. 939–949.
- [40] Alexander Strehl and Joydeep Ghosh. “Cluster ensembles—a knowledge reuse framework for combining multiple partitions”. In: *Journal of machine learning research* 3.Dec (2002), pp. 583–617.
- [41] Lei Tang, Xufei Wang, and Huan Liu. “Community detection via heterogeneous interaction analysis”. In: *Data mining and knowledge discovery* 25.1 (2012), pp. 1–33.
- [42] Lei Tang, Xufei Wang, and Huan Liu. “Uncovering groups via heterogeneous interaction analysis”. In: *2009 Ninth IEEE International Conference on Data Mining*. IEEE. 2009, pp. 503–512.
- [43] Wei Tang, Zhengdong Lu, and Inderjit S Dhillon. “Clustering with multiple graphs”. In: *2009 Ninth IEEE International Conference on Data Mining*. IEEE. 2009, pp. 1016–1021.
- [44] Dane Taylor, Rajmonda S Caceres, and Peter J Mucha. “Super-resolution community detection for layer-aggregated multilayer networks”. In: *Physical Review X* 7.3 (2017), p. 031056.
- [45] Dane Taylor et al. “Enhanced detectability of community structure in multilayer networks through layer aggregation”. In: *Physical review letters* 116.22 (2016), p. 228301.

- [46] James D Wilson et al. “Community extraction in multilayer networks with heterogeneous community structure”. In: *The Journal of Machine Learning Research* 18.1 (2017), pp. 5458–5506.
- [47] Robert Winkler. *Introduction to Bayesian Inference and Decision*. Probabilistic Publishing, Gainesville, 2003.
- [48] Rongkai Xia et al. “Robust multi-view spectral clustering via low-rank and sparse decomposition”. In: *Proceedings of the AAAI conference on artificial intelligence*. Vol. 28. 1. 2014.
- [49] Zhiping Zeng et al. “Coherent closed quasi-clique discovery from large dense graph databases”. In: *Proceedings of the 12th ACM SIGKDD international conference on Knowledge discovery and data mining*. 2006, pp. 797–802.
- [50] Kun Zhan et al. “Graph learning for multiview clustering”. In: *IEEE transactions on cybernetics* 48.10 (2017), pp. 2887–2895.
- [51] Kun Zhan et al. “Graph structure fusion for multiview clustering”. In: *IEEE Transactions on Knowledge and Data Engineering* 31.10 (2018), pp. 1984–1993.
- [52] Kun Zhan et al. “Multiview consensus graph clustering”. In: *IEEE Transactions on Image Processing* 28.3 (2018), pp. 1261–1270.
- [53] Dengyong Zhou and Christopher JC Burges. “Spectral clustering and transductive learning with multiple views”. In: *Proceedings of the 24th international conference on Machine learning*. 2007, pp. 1159–1166.
- [54] Linlin Zong et al. “Weighted multi-view spectral clustering based on spectral perturbation”. In: *Proceedings of the AAAI Conference on Artificial Intelligence*. Vol. 32. 1. 2018.



# Supplementary Material: Louvain-like Methods for Community Detection in Multiplex Networks

Sara Venturini\*, Andrea Cristofari†, Francesco Rinaldi‡, Francesco Tudisco§

## 1 Detailed Description of the Real-World Networks

Here is a detailed description of the five real-world networks used in Section 5.3.

- *3sources* is a text dataset of articles from three online news sources (BBC, Reuters, and The Guardian), one for each layer, which have been manually assigned to one of six topical labels: business, entertainment, health, politics, sport and technology [2, 3].
- *BBCSport* is a news dataset of sports articles with five annotated topic labels. The two layers are created splitting each document into segments and assigning them randomly to layers [2].
- *Cora* is a citation dataset of research papers labeled with seven classes. The first layer is a citation network, whereas the second one is built on documents features [4].
- *UCI* is a dataset of features of handwritten digits (0-9). These digits are represented in terms of six different feature sets, forming the layers: Fourier coefficients of the character shapes, profile correlations, Karhunen-Love coefficients, pixel averages, Zernike moments and morphological features [1, 3].
- *Wikipedia* is a dataset of wikipedia articles classified in ten categories: art & architecture, biology, geography, history, literature & theatre, media, music, royalty & nobility, sport & recreation, Warfare. These categories are assigned to both the text and image components of each article, corresponding to the two layers [5].

All the layers built from feature sets are formed by means of a symmetrized  $k$ -nearest neighbor graph with  $k = 10$ , based on the Pearson linear correlation between nodes, i.e., the higher the correlation the smaller the nodes distance. Thus, if  $N_k(u)$  denotes the set of  $k$  nodes that have highest correlation with node  $u$ , to each node  $u$  we connect all nodes in the set

$$N_k(u) \cup \{v : u \in N_k(v)\}.$$

The main properties of the various multilayer networks are reported in Table 1.

\*Department of Mathematics “Tullio Levi-Civita”, University of Padova, 35121 Padova, Italy (sara.venturini@math.unipd.it)

†Department of Mathematics “Tullio Levi-Civita”, University of Padova, 35121 Padova, Italy (andrea.cristofari@unipd.it)

‡Department of Mathematics “Tullio Levi-Civita”, University of Padova, 35121 Padova, Italy (rinaldi@math.unipd.it)

§School of Mathematics, Gran Sasso Science Institute, Italy, (francesco.tudisco@gssi.it)

A. Cristofari, F. Rinaldi and F. Tudisco contributed equally to this work.

Table 1: Basic statistics for the real-world datasets. For each dataset it shows the number of nodes, the number of communities, the size of the communities, the number of layers and, for each layer, the number of edges  $|E|$ , the edge density  $\delta$  and the average and standard deviation of the nodes' degrees,  $\langle k \rangle$  and  $\sigma$ , respectively.

	3sources				BBCSport				cora				UCI				Wikipedia			
# nodes	169				544				2708				2000				693			
# comm.	6				5				7				10				10			
Comm. size	56,21,11,18,51,12				62,104,193,124,61				298,418,818, 426,217,180,351				200 each				34,88,96,85,65,58,51,41,71,104			
# layers	3				2				2				6				2			
	E	$\delta$	$\langle k \rangle$	$\sigma$	E	$\delta$	$\langle k \rangle$	$\sigma$	E	$\delta$	$\langle k \rangle$	$\sigma$	E	$\delta$	$\langle k \rangle$	$\sigma$	E	$\delta$	$\langle k \rangle$	$\sigma$
I layer	1168	0.04	12.82	3.37	4075	0.01	13.98	5.22	5278	7.2e-4	3.90	5.23	14447	3.4e-3	13.45	3.54	5606	0.01	15.18	5.37
II layer	1223	0.04	13.47	4.55	4127	0.01	14.17	6.42	21273	2.7e-3	14.71	9.52	14600	3.4e-3	13.60	3.70	5385	0.01	28.83	5.37
III layer	1272	0.04	14.05	5.13	-	-	-	-	-	-	-	-	14498	3.4e-3	13.50	3.48	-	-	-	-
IV layer	-	-	-	-	-	-	-	-	-	-	-	-	12729	2.9e-3	11.73	1.67	-	-	-	-
V layer	-	-	-	-	-	-	-	-	-	-	-	-	14561	3.4e-3	13.56	3.73	-	-	-	-
VI layer	-	-	-	-	-	-	-	-	-	-	-	-	14421	3.4e-3	13.42	3.43	-	-	-	-

## 2 Synthetic Networks via SBM with communities of different sizes

In order to verify how the difference in the size of the communities can influence the performances, we tested the methods on networks with communities of different sizes. In particular, we generated networks by the SBM with 3 communities of 100, 150 and 200 nodes, respectively. We keep the same values for  $p$  and  $p/q$ , and we studied the same cases. Results are shown in Figures 1 and 2: 1(a) two informative layers, 1(b) three informative layers, 2(a) two informative layers and one noisy layer, 2(b) two informative layers and two noise ones. We do not report the results of IM, because it achieves very low results with respect to the others, mostly including all the nodes in just one community. In general, we see that the performances of the methods are not really affected by the dimension of the communities.

## 3 Analysis of the parameter $\gamma$

In the definition of the functions  $F_-$  and  $F_+$ , we set  $\gamma = \{0.1, 0.3, 0.5, 0.7, 0.9\}$ . Here, we analyze the NMI results of the methods as the parameter  $\gamma$  changes. The analysis for the Accuracy results are similar. We report heatmaps related to the different networks used in the tests, that is

- Synthetic Networks via SBM used in Section 5.1 (see Figures 3 for the informative cases and 4 for the noisy cases),
- Synthetic Networks via LFR used in Section 5.2 (see Figures 5 for the informative cases and 6 for the noisy cases),
- Real-World Networks used in Section 5.3 (see Figure 7 for both informative and noisy case).

As we can easily see by taking a look at the figures, NMI values do not change that much when the  $\gamma$  parameter changes.

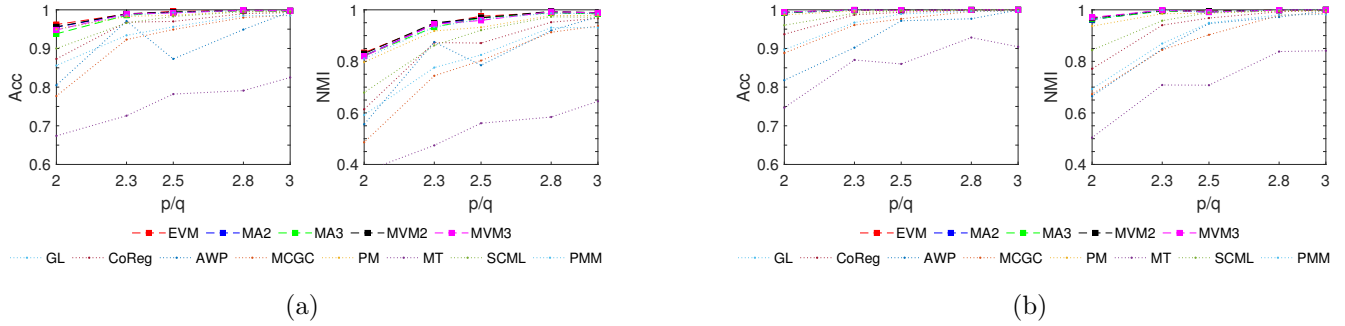


Figure 1: The figure consists of two pairs (a) and (b) of line plots, showing the average values of accuracy and NMI over 10 random networks sampled from SBM with equally distributed informative layers (2 layers (a) and 3 layers (b)), with three communities of 100, 150 and 200 nodes, respectively, each having internal edge probability equal to  $p = 0.1$  and cross-community edge probability  $q$  varying so that  $p/q \in \{2, 2.3, 2.5, 2.8, 3\}$ .

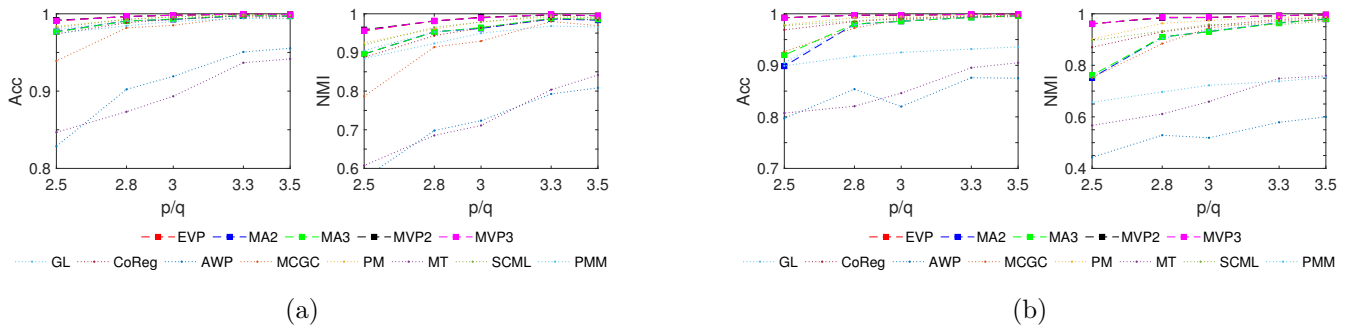


Figure 2: The figure consists of two pairs (a) and (b) of line plots, showing the average values of accuracy and NMI over 10 random networks sampled from the SBM with both informative and noisy layers (two informative and one noisy in (a) and two informative and two noisy in (b)). The informative layers have three communities of 100, 150 and 200 nodes, respectively, each having internal edge probability equal to  $p = 0.1$  and cross-community edge probability  $q$  varying so that  $p/q \in \{2.5, 2.8, 3, 3.3, 3.5\}$ . The noisy layers are SBM graphs with  $p = q = 0.1$ .

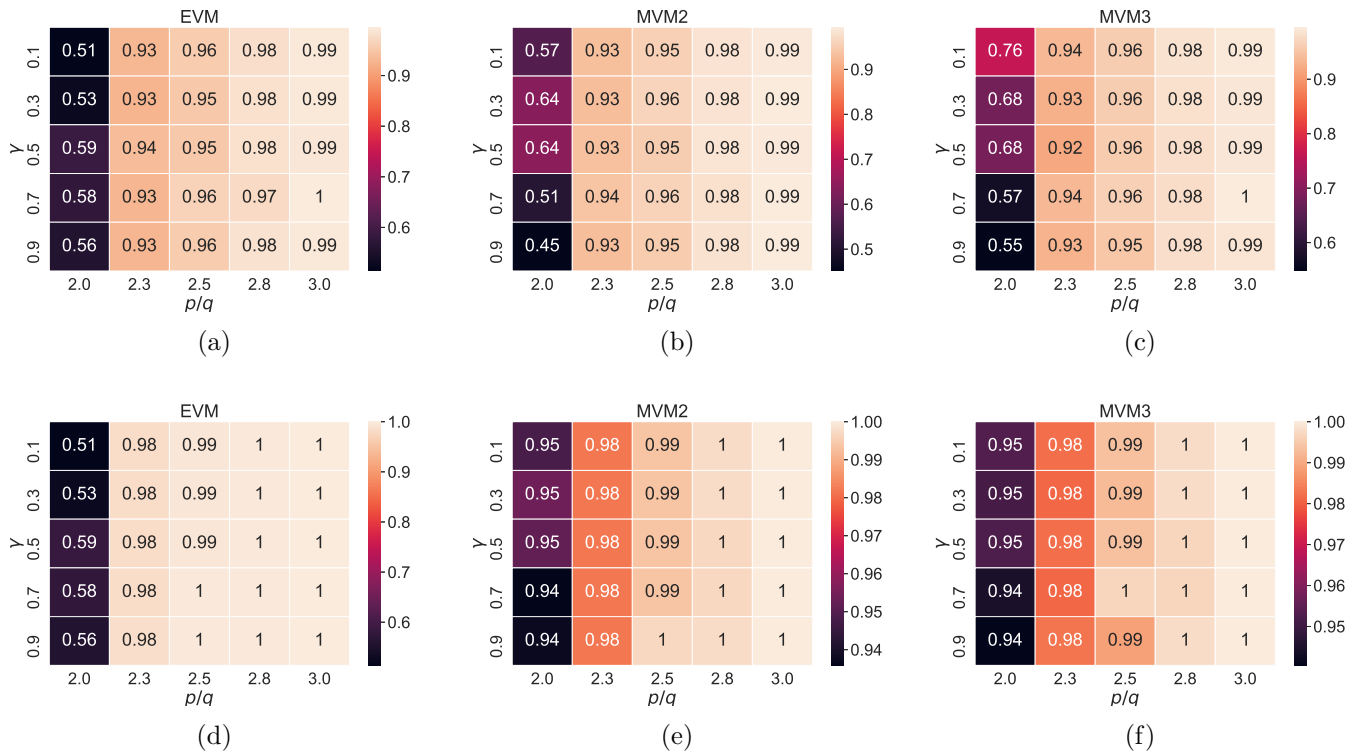


Figure 3: The image is composed by two triplets of heatmaps. They represent the NMI results as the parameter  $\gamma$  changes for networks generated by the SBM in the informative cases (2 layers (a),(b),(c) and 3 layers (d),(e),(f)). (a) and (d) refer to EVM, (b) and (e) refer to MVM2, (c) and (f) refer to MVM3.

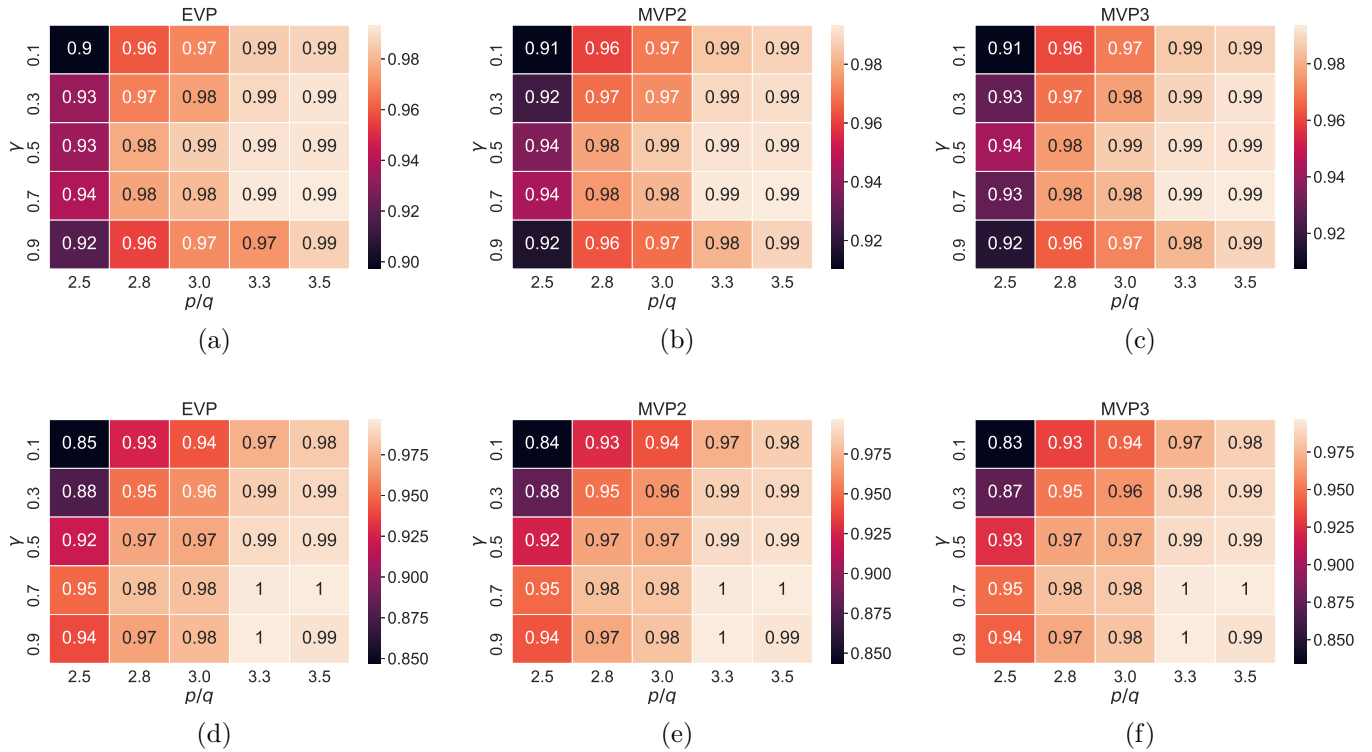


Figure 4: The image is composed by two triplets of heatmaps. They represent the NMI results as the parameter  $\gamma$  changes for networks generated by the SBM in the noisy cases (two informative and one noisy in (a),(b),(c), and two informative and two noisy in (d),(e),(f)). (a) and (d) refer to EVP, (b) and (e) refer to MVP2, (c) and (f) refer to MVP3.

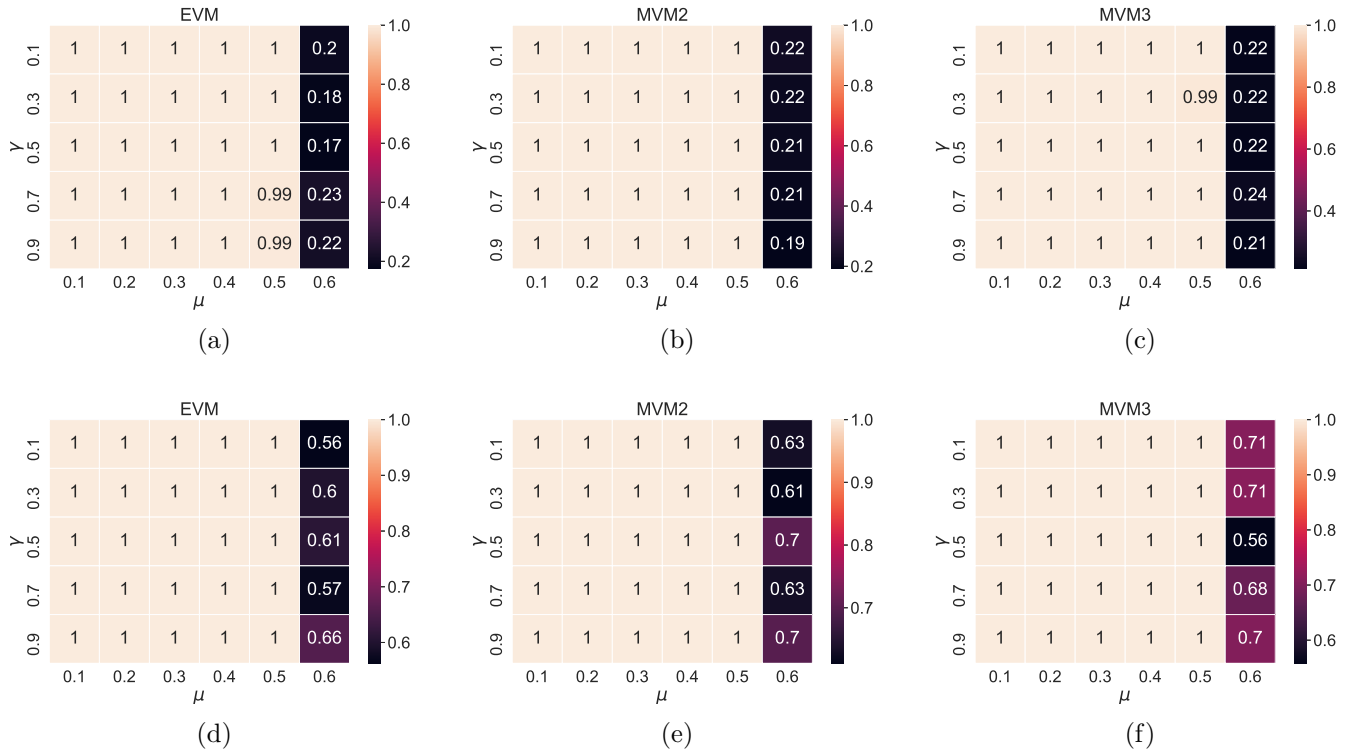


Figure 5: The image is composed by two triplets of heatmaps. They represent the NMI results as the parameter  $\gamma$  changes for networks generated by the LFR benchmark in the informative cases (2 layers (a),(b),(c) and 3 layers (d),(e),(f)). (a) and (d) refer to EVM, (b) and (e) refer to MVM2, (c) and (f) refer to MVM3.

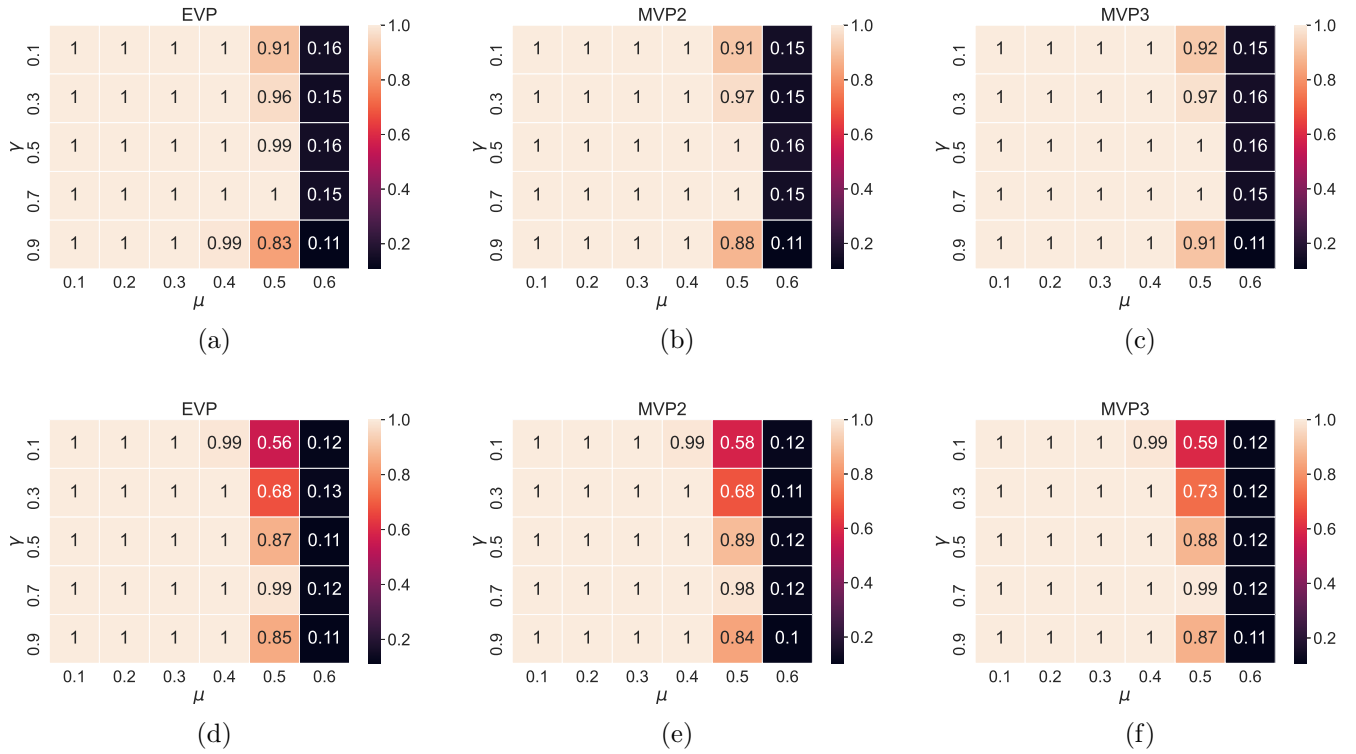


Figure 6: The image is composed by two triplets of heatmaps. They represent the NMI results as the parameter  $\gamma$  changes for networks generated by the LFR benchmark in the noisy cases (two informative and one noisy in (a),(b),(c), and two informative and two noisy in (d),(e),(f)). (a) and (d) refer to EVP, (b) and (e) refer to MVP2, (c) and (f) refer to MVP3.

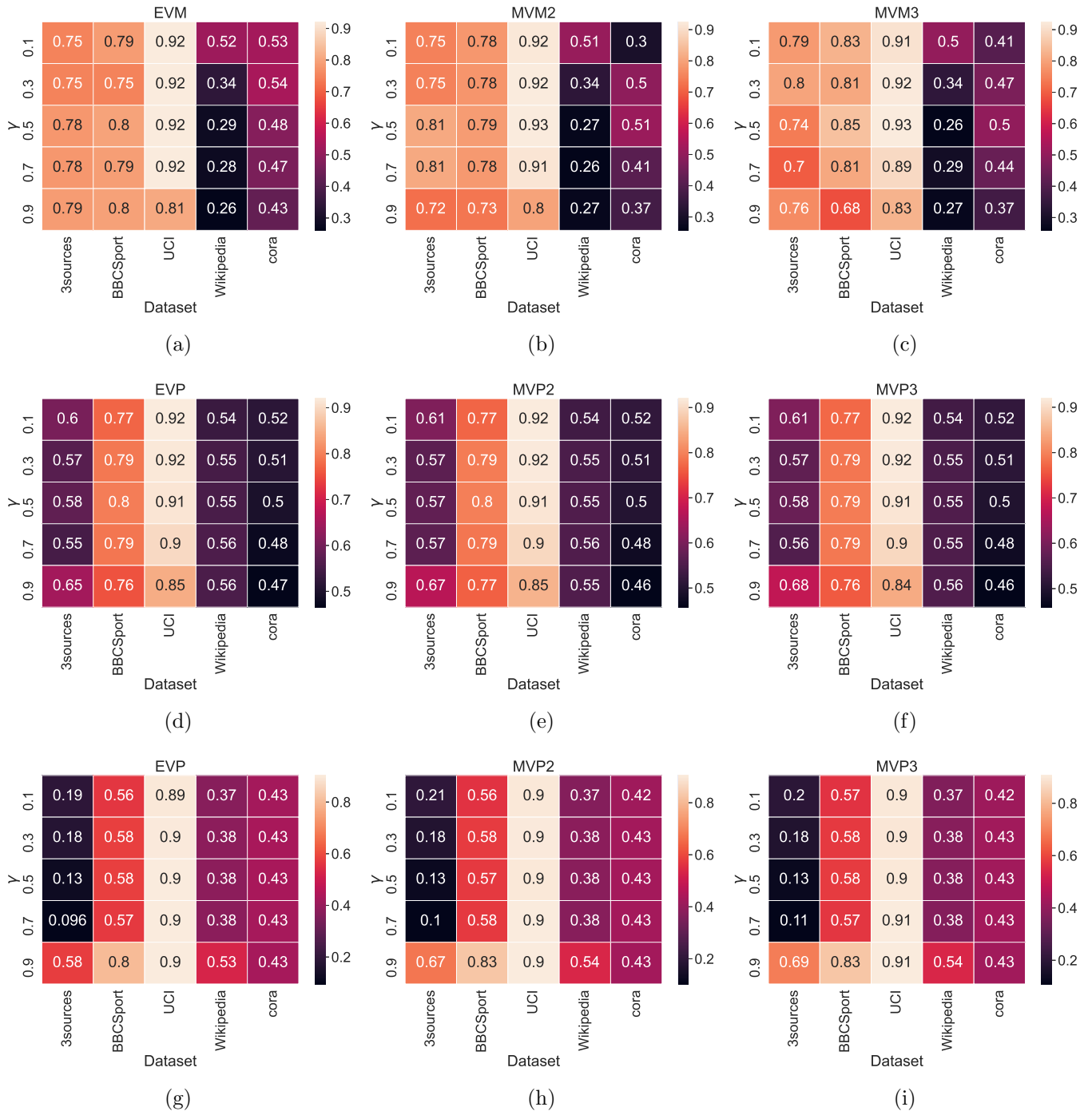


Figure 7: The figure consists of three triplets of heatmaps, representing the NMI score for the EVM, EVP, MVM and MVP methods on the real-world datasets listed in Table 1, as the parameter  $\gamma$  in the definition of the variance-aware multilayer cost functions  $F_{\pm}$  varies. For each dataset we consider both the informative case (all informative layers (a),(b),(c)), the noisy cases (setting one (d),(e),(f) and setting two (g),(h),(i)) (a) refer to EVM, (b) refer to MVM2, (c) refer to MVM3; (d) and (g) refer to EVP, (e) and (h) refer to MVP2, (f) and (i) refer to MVP3.



## References

- [1] Dheeru Dua and Casey Graff. *UCI Machine Learning Repository – Multiple Features Data Set*. 2017. URL: <https://archive.ics.uci.edu/ml/datasets/Multiple+Features>.
- [2] Derek Greene and Pádraig Cunningham. “A matrix factorization approach for integrating multiple data views”. In: *Joint European conference on machine learning and knowledge discovery in databases*. Springer. 2009, pp. 423–438.
- [3] Jialu Liu et al. “Multi-view clustering via joint nonnegative matrix factorization”. In: *Proceedings of the 2013 SIAM International Conference on Data Mining*. SIAM. 2013, pp. 252–260.
- [4] Andrew Kachites McCallum et al. “Automating the construction of internet portals with machine learning”. In: *Information Retrieval* 3.2 (2000), pp. 127–163.
- [5] Nikhil Rasiwasia et al. “A new approach to cross-modal multimedia retrieval”. In: *Proceedings of the 18th ACM international conference on Multimedia*. 2010, pp. 251–260.